

AN EXPERIMENTAL METHOD FOR THE INVESTIGATION  
OF SUBSONIC STALL FLUTTER IN GAS TURBINE  
ENGINE FANS AND COMPRESSORS

by

William Ward Copenhaver

Thesis submitted to the Graduate Faculty of the  
Virginia Polytechnic Institute and State University  
in partial fulfillment of the requirements for the degree of

MASTER OF SCIENCE

in

Mechanical Engineering

APPROVED:

---

W. F. O'Brien

---

H. L. Moses

---

L. D. Mitchell

September 1978

Blacksburg, Virginia

#### ACKNOWLEDGMENTS

The author expresses appreciation to the members of his advisory committee: Professors W. F. O'Brien, H. L. Moses and L. D. Mitchell.

The assistance and guidance of \_\_\_\_\_ was especially appreciated.

The author thanks \_\_\_\_\_ and \_\_\_\_\_ for their aid in photographic technique development, \_\_\_\_\_ and \_\_\_\_\_ for aid and understanding in purchasing difficulties, and \_\_\_\_\_ for her excellent typing of this thesis.

Lastly, the author would like to thank his parents and his wife's parents for their financial and moral support during his college career. Especial thanks goes to the author's wife, \_\_\_\_\_, for her unending concern and understanding during the past four years.

TABLE OF CONTENTS

	<u>Page</u>
ACKNOWLEDGMENTS. . . . .	ii
LIST OF FIGURES. . . . .	v
NOMENCLATURE . . . . .	vii
INTRODUCTION . . . . .	1
REVIEW OF LITERATURE . . . . .	4
FLUTTER FUNDAMENTALS . . . . .	7
EXPERIMENTAL APPARATUS . . . . .	13
Requirements . . . . .	13
Blade Flutter Test Facility. . . . .	14
Photographic Method. . . . .	18
Acoustical Method. . . . .	21
Flow Measurement . . . . .	21
RESULTS. . . . .	25
Experimental Procedure . . . . .	25
Experimental Results . . . . .	26
DISCUSSION OF RESULTS. . . . .	38
Summary of Results . . . . .	40
CONCLUSIONS. . . . .	41
RECOMMENDATIONS. . . . .	42
LITERATURE CITED . . . . .	43
APPENDIX 1 . . . . .	45
List of Equipment. . . . .	46
APPENDIX 2 . . . . .	47

TABLE OF CONTENTS, cont.

	<u>Page</u>
Flow Relative Velocity Comparisons . . . . .	48
Real-Time Analyzer Results . . . . .	49
VITA . . . . .	50
ABSTRACT	

## LIST OF FIGURES

<u>Figure</u>		<u>Page</u>
1	Example of Compressor Flutter Regions. . . . .	1
2	Example of Stress Rise Results . . . . .	8
3	Flutter Boundaries . . . . .	9
4	Geometry for Blade Flutter Analysis. . . . .	10
5	Cascade Parameters for Flutter Analysis. . . . .	12
6	View of Inlet of Test Fan. . . . .	15
7	View of Drive System on Test Fan . . . . .	16
8	Flutter Test Facility Schematic. . . . .	17
9	View of Hatch to Aid in Varying Blade Stagger Angle. . .	19
10	View of Test Fan Blade . . . . .	20
11	View of Photographic Equipment . . . . .	22
12	View of Test Fan Instrumentation . . . . .	23
13	Velocity Triangle. . . . .	28
14	Stall Flutter Speed Comparison . . . . .	29
15	Comparison Between Sonic Waveform at 2000 RPM and 3000 RPM for 65-Degree Blade Stagger Angle. . . . .	30
16	Comparison Between Sonic Waveform at 2000 RPM and 3000 RPM for 60-Degree Blade Stagger Angle. . . . .	31
17	Sonic Waveform and Blade Photograph at 2100 RPM for a Blade Stagger Angle of 55 Degrees. . . . .	32
18	Sonic Waveform and Blade Photograph at 2800 RPM for a Blade Stagger Angle of 55 Degrees (Flutter Present). . .	33

LIST OF FIGURES, cont.

<u>Figure</u>		<u>Page</u>
19	Sonic Waveform and Blade Photograph at 1500 RPM for a Blade Stagger Angle of 50 Degrees. . . . .	34
20	Sonic Waveform and Blade Photograph at 2500 RPM for a Blade Stagger Angle of 50 Degrees (Flutter Present). . .	35
21	Sonic Waveform and Blade Photograph at 1600 RPM for a Blade Stagger Angle of 45 Degrees. . . . .	36
22	Sonic Waveform and Blade Photograph at 2500 RPM for a Blade Stagger Angle of 45 Degrees (Flutter Present). . .	37
23	Flow Relative Velocity Comparisons. . . . .	48
24	Frequency Components of Test Fan Sonic Output . . . . .	49

## NOMENCLATURE

- $b$  = length of the blade semichord
- $b_a$  = distance from the shear center to the center of gravity
- $b_h$  = vertical deflection of blade measured at the elastic axis
- $c$  = blade chord length =  $2b$
- $I_Y$  = mass moment of inertia about the shear center of the blade
- $K_Y$  = blade torsional stiffness
- $K_h$  = blade bending stiffness
- $L$  = lift on the blade
- $M$  = moment on the blade
- $m$  = unit span-wise mass of the blade
- $Q_h$  = unsteady aerodynamic forces due to plunging of the blade
- $Q_Y$  = unsteady aerodynamic forces due to the pitching of the blade
- $s$  = interblade spacing
- $U$  = cascade rotation speed
- $V$  = relative velocity
- $\alpha$  = angle of incidence
- $\omega$  = blade vibratory frequency
- $\gamma$  = angle of blade twist
- $\lambda$  = blade stagger angle
- $\beta$  = flow angle
- $\phi$  = interblade phase angle

## INTRODUCTION

Flutter, an aeroelastic phenomenon first associated with aircraft wings, has also become a problem in present day gas turbine engine compressors and fans. The problem arises due to the need for lighter, thinner blading for increased thrust-to-weight ratio in aircraft gas turbines. With thinner, lighter blades in compressors, the dynamic effect of the air on the blades becomes a controlling factor in the blade stability.

The unsteady phenomenon of flutter occurs when the vectorial sum of mechanical damping of the blades and aerodynamic damping of the airflow becomes zero. At this point, the blades experience severe self-induced oscillations. These oscillations of fan and compressor blading reduce gas turbine efficiency and increase blade fatigue damage. Therefore, this makes flutter an undesirable phenomenon in aircraft gas turbines.

Flutter occurs in four ranges of gas turbine operation as shown on the compressor map in Fig. 1 and outlined by Mikolajczak [1]\*.

(1) Supersonic unstalled range: This type of flutter occurs when the full span of the compressor blade has air flow that is operating at supersonic speeds relative to the blades. This can occur at or near the design point of operation. This occurrence places a limit on the speed of operation and, therefore, the maximum pressure rise of the machine.

(2) Supersonic stalled range: Flutter occurs as before in the supersonic relative velocity region, but at or near the surge limit of compressor operation.

(3) Choke range: Flutter occurs when the compressor is operating

---

\*Numbers in brackets indicate references listed at the end of thesis.

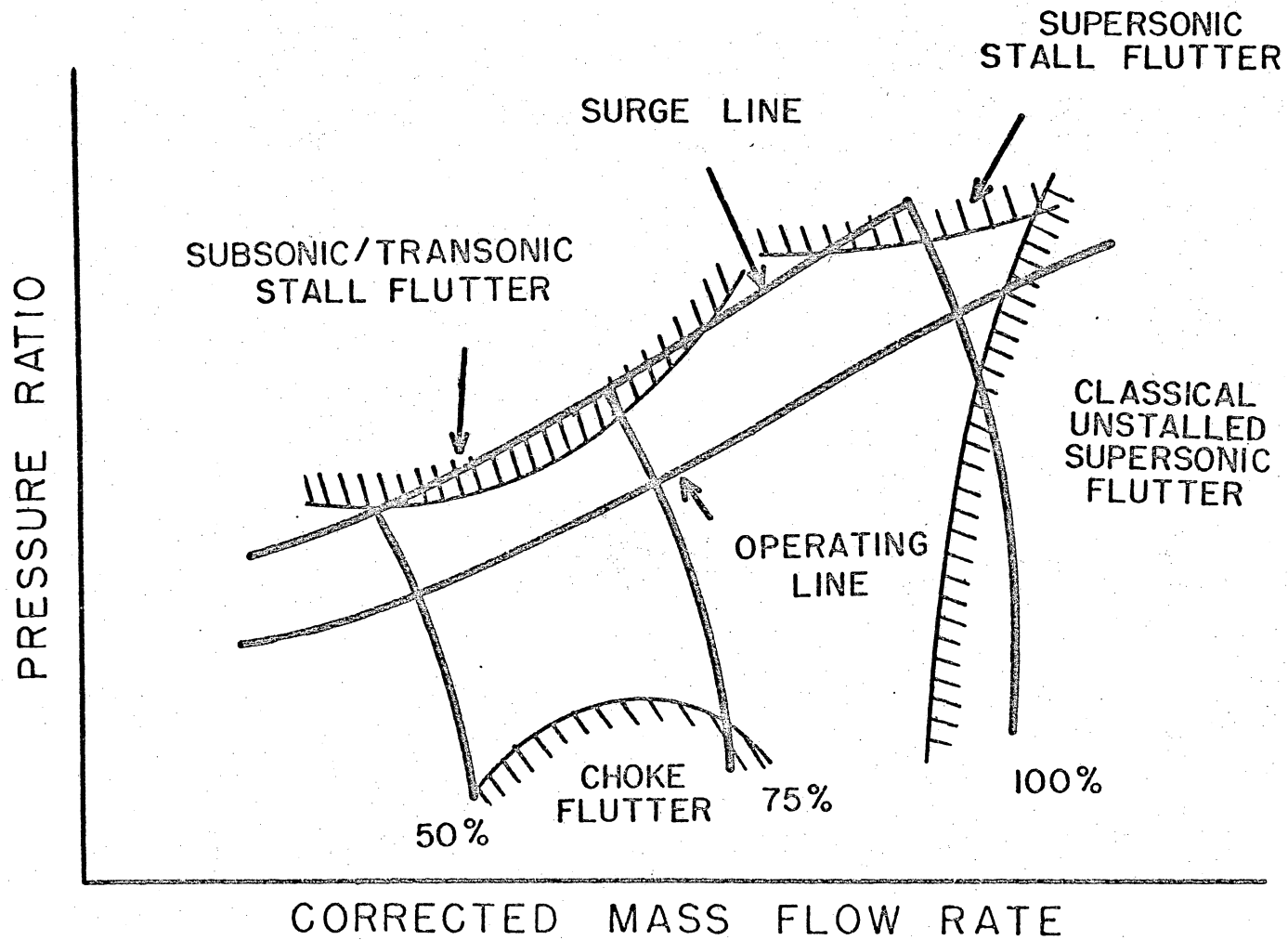


FIGURE 1. EXAMPLE OF COMPRESSOR FLUTTER REGIONS  
(FROM REF. 1)

at high-flow in or near the choking region and the flow is transonic over most of the blade chord.

(4) Subsonic stalled range. Flutter occurs when the compressor is operating in the near-surge range and the flow over the blades is subsonic; as, for example, at part speed for a high speed fan. This speed may be within the design range of operation, and therefore cause a reduction in compressor performance and possible blade damage.

Since subsonic stalled flutter occurs at low rotor speeds and blade velocities, it may be produced in a relatively low-speed experimental apparatus. For this reason and because of the importance of the subject, subsonic stalled flutter was chosen as the subject for this investigation. This thesis provides data which are intended to aid in the modification of present aircraft wing prediction techniques so that these techniques may be used to predict effects in blade cascades. This modified technique should accommodate adjacent blade interactions and end wall effects in turbomachines.

An experimental method for the investigation of the stall flutter phenomenon in a rotating fan is presented. This experimental technique involves the development of a special low-speed rotating fan. The fan has design parameters equivalent to present day high-speed compressors and will flutter in low-speed operation. This apparatus was designed so that the occurrence of subsonic stall flutter can be investigated employing photographic techniques. Acoustical and strain gauge stall flutter information can also be obtained from this apparatus.

## REVIEW OF LITERATURE

The first experimental methods for the investigation of the flutter phenomenon in turbomachines involved stationary cascades. N. D. Tikhonov [2] conducted a study on a cascade of compressor blades. The study involved determining the influence of cascade parameters on flutter. The experimental apparatus consisted of an aerodynamic tube used for creating air flows around cascades with a wide range of flow velocities and angles of attack. F. O. Carta [3] performed experiments on a subsonic cascade oscillating near stall. The experimental apparatus contained an oscillating cascade wind tunnel with airfoils fitted with high-response and hot film pressure transducers. The effects of interblade phase angle, frequency of oscillation and free-stream velocities on flutter were investigated. The results showed that the change of interblade phase angle radically alters the character of the unsteady blade loading.

Additional cascade experimentation was performed by S. Yashima and H. Tanaka [4]. Their experimental apparatus involved a water tunnel with a linear cascade of 11 blades. The blades were forced to vibrate in a torsional mode about their rotational axes at the same amplitude and constant interblade phase angle. A black-ink flow visualization technique was used to determine the separation point on the blade. Also, the unsteady moment acting on the blade was measured using strain gauges

Because of the lack of centrifugal effects in cascade tests, rotating experiments have been conducted to verify analytic prediction techniques. Mikolajczak [1] advanced the experimental technique by the investigation of actual rotating machinery. With a rotating shrouded fan, and through

the use of an optical technique known as holography, the mode shapes of the vibrating blades were determined. B. S. Hockley, et al [5] also used double pulse holography to measure vibratory modes of a rotating fan. Jeffers and Meece [6] developed an on-rotor test program to investigate the stall flutter problems of the F100 Turbofan engines. The test involved placing the engine in a test cell to control atmospheric conditions. Compressor blade vibratory response was determined from blade-mounted strain gauges. These gauges transmitted electrical signals through slip rings to stationary FM recording equipment. Through a blade redesign the occurrence of stall flutter in the engine operation zone was reduced. It was noted that analytical methods fell short in the prediction of stall flutter in the F100 Turbofan.

Another experimental method in stall flutter research was developed by Banerjee and Rao [7]. Their experimental apparatus contained a two-bladed rotor with blade-mounted piezoelectric crystals. Some of the crystals were used to excite the blades and others were used to measure the response. The response was then transmitted through slip rings to a stationary frequency analyzer.

FM telemetry techniques in the investigation of on-rotor stall flutter were developed due to speed limitations of slip rings. Daws [8] and Sparks [9] report success in the use of blade-mounted strain gauges in the measurement of flutter on a rotating cascade. Data were transmitted from the rotor by FM telemetry. Problems were reported in the level sensitivity of the torsional channel. Adler [10] reports on advantages and limitations of on-rotor telemetry.

H. Stargardter [11] employed an optical technique for the measurement of flutter motion. These measurements were made with small blade-mounted mirrors that reflect laser light once per revolution. Through this method, vibration amplitude, phase and frequency of rotating compressor blades were determined. Bien and Camac [12] used optical interferometric techniques to measure frequency and amplitude of vibration of a rotating element. W. C. Nieberding and J. L. Pollack [13] explored two methods of optical detection of the onset of blade flutter in fan blades of an aircraft gas turbine. One method involved photoelectric scanning of blade tip motion. Time between subsequent passing of blade tips was measured to determine the presence of blade flutter. The second method was that of stroboscopic imagery. Through the use of a short duration pulse once per revolution, the rotor motion was apparently arrested, and one blade tip was monitored for flutter motion. Both methods gave real time histories of fan blade flutter.

## FLUTTER FUNDAMENTALS

At this point a basic theory for the mechanics of stall flutter will be developed to aid in showing the purpose and direction of this thesis.

Early methods of avoiding stall flutter in compressors were developed through stress rise tests [14]. These tests involved measurements of stress in turbomachinery blading due to the increase in inlet flow velocity and angle of incidence. These results generated the curves of the type in Fig. 2. These curves were then nondimensionalized and converted to the type of curve shown in Fig. 3, where  $b$  is one-half of the blade cord length,  $\omega$  is the blade vibratory frequency,  $V$  is the relative velocity of the inlet flow and  $\alpha$  is the angle of incidence of that flow. As can be seen, reduction of a given blade's vibratory frequency causes the blade to enter the unstable region for a high angle of incidence. Present turbomachine blading, with their reduced weight and thickness, may enter into this unstable range during normal operating conditions.

Because of the increasing cost and time for development of a test compressor for these stress rise tests, an analytic method for the prediction of flutter has become desirable. Flutter prediction involves the determination of the flutter speed, the rotational speed at which flutter occurs, and the frequency at which the blades vibrate, called the flutter frequency. The basic theory underlying an analytical method can be explained through the use of the model shown in Fig. 4, where  $b$  is one-half of the blade cord length,  $b_h$  is the vertical blade deflection,  $\gamma$ ,  $M$ ,  $L$  are the angle of twist, moment and lift, respectively, on the blade during flutter, and  $b_a$  is the distance from the elastic axis to the center of gravity of the blade. From Fig. 4, the equation of motion in

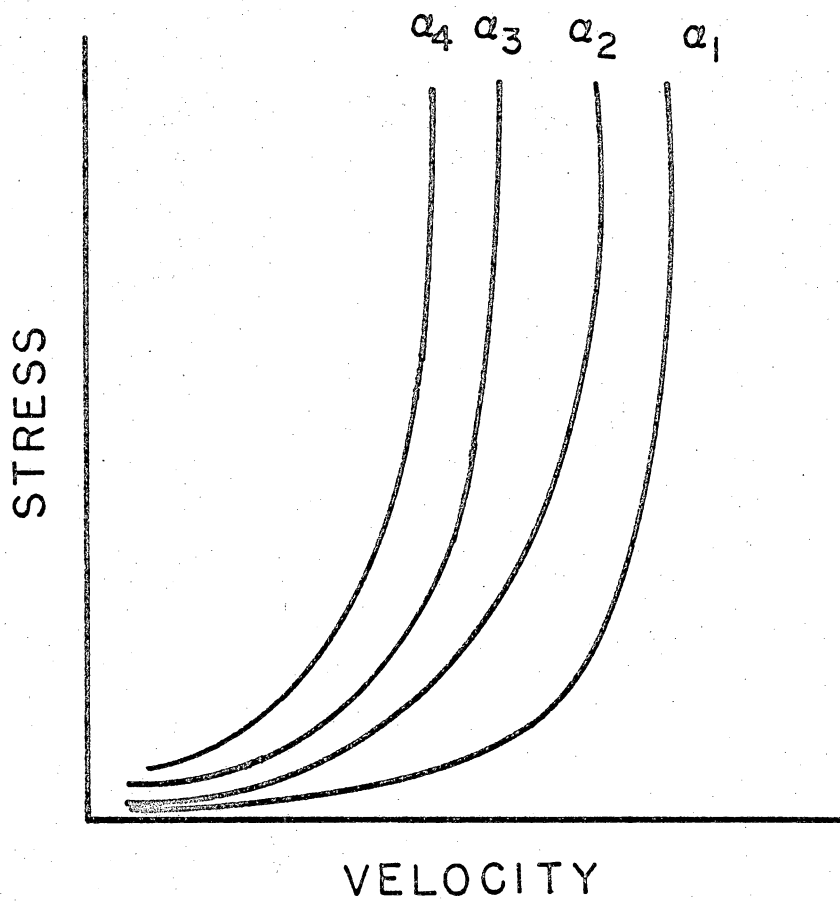


FIGURE 2. EXAMPLE OF STRESS RISE RESULTS  
(FROM REF. 14)

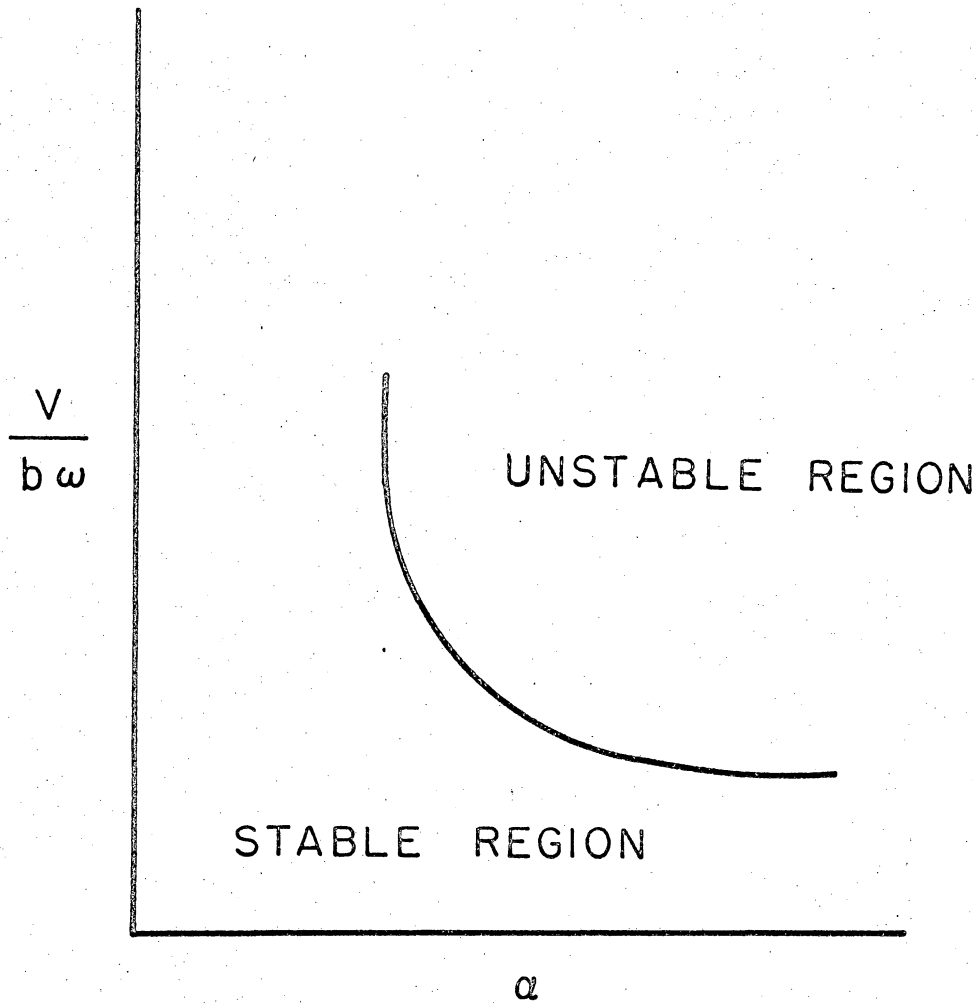


FIGURE 3. FLUTTER BOUNDARIES  
(FROM REF. 14)

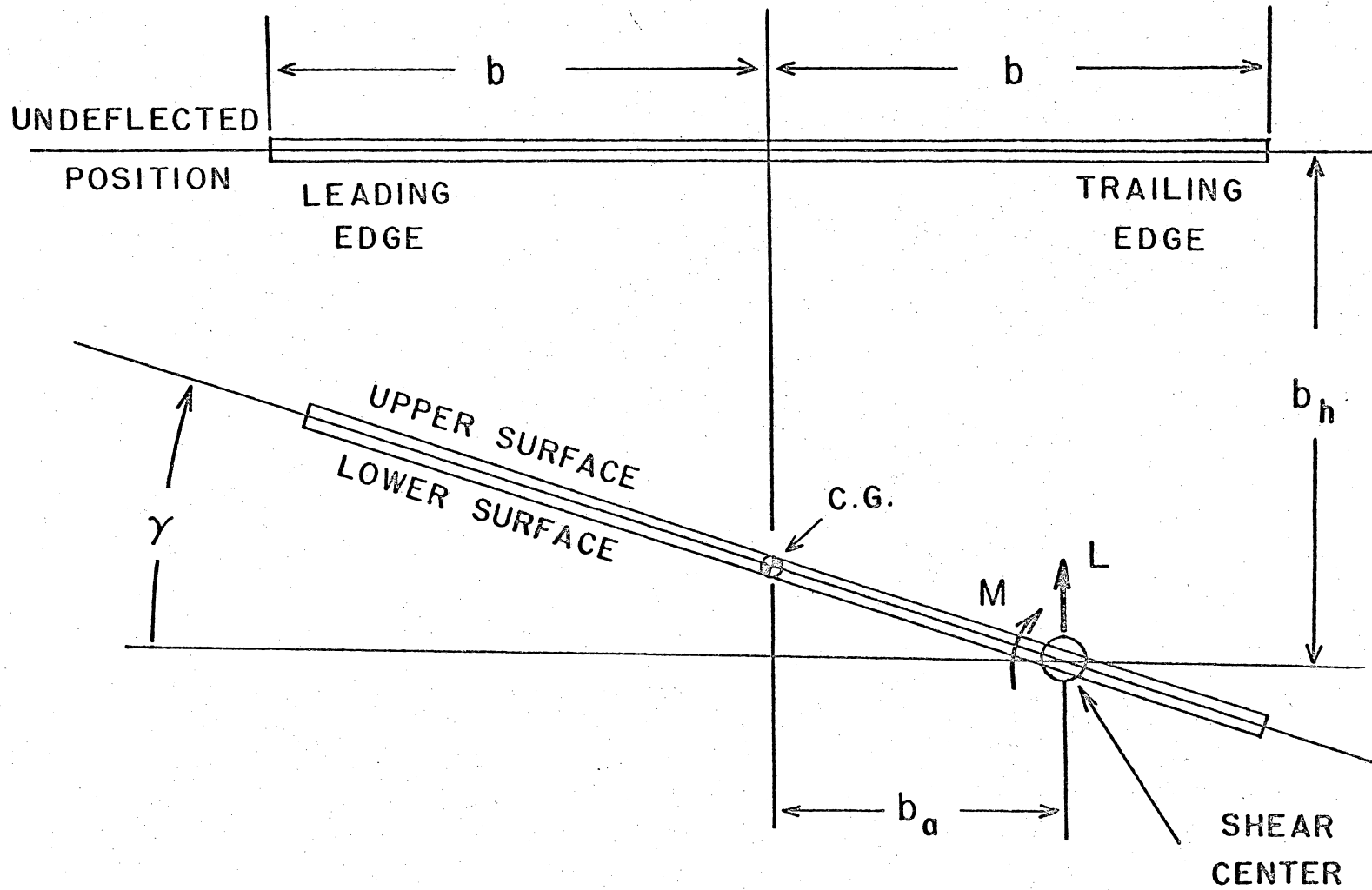


FIGURE 4. GEOMETRY FOR BLADE FLUTTER ANALYSIS

bending can be determined as

$$m\ddot{b}_h + K_h b_h - m b_a \ddot{\gamma} = Q_h.$$

The equation for torsional motion is

$$I_Y \ddot{\gamma} + K_Y \gamma - m b_a \ddot{b}_h = Q_Y$$

where the unit spanwise mass and the mass moment of inertia about the shear center are represented by  $m$  and  $I_Y$ , respectively.  $Q_h$  represents the unsteady aerodynamic forces due to plunging motion of the blade and  $Q_Y$  represents the unsteady aerodynamic forces due to pitching motion of the blade.

The evaluation of the term  $Q_Y$  represents the greatest challenge in the development of analytical theory for the prediction of stall flutter. To make an accurate prediction of stall flutter speed and frequency,  $Q_Y$  must represent the unsteady forces associated with separation and possible reattachment of the airflow. These unsteady forces are direct functions of such cascade parameters as interblade spacing  $s$ , blade stagger angle  $\lambda$  and interblade phase angle  $\phi$  as shown in Fig. 5.

The purpose of this thesis is to develop an experimental method for the investigation of the effect of cascade parameters on flutter speed and frequency in a rotating fan. These experimental results may then aid in the verification and/or modification of an analytic model for stall flutter.



## EXPERIMENTAL APPARATUS

### Requirements

To study the occurrence of stall flutter in aircraft engine fans and compressors, an experimental apparatus must be designed with design parameters which may be related to aircraft turbofans. It also must be able to accommodate experimental methods for the investigation of stall flutter. Previous experiments have shown that a stationary cascade of blades lacks centrifugal effects which are necessary in the investigation of turbofan stall flutter. Therefore, a rotational cascade of blades was judged to be necessary.

Since stall flutter occurs in the subsonic range of operation, a medium range rotational speed fan (10,000 RPM top speed) was designed for the investigation. Previous investigations by Daws [8] and Sparks [9] encountered problems in obtaining the necessary speed ranges for a complete investigation of stall flutter. For a detailed investigation of stall flutter, the cascade must have a sufficiently variable speed drive system to cover the full range of flutter speeds.

Stall flutter has been defined as a self-induced blade vibration due to the interaction of the aerodynamics of the flow and the mechanics of the blade. To assure that there is no external aerodynamic force acting on the cascade blades, they should be positioned so as to reduce the effects of any upstream wakes in the flow. The interaction between aerodynamics and mechanics is controlled by such cascade parameters as solidity,  $c/s$ , and blade stagger angle,  $\lambda$ . The effects of these parameters must be included in an investigation of stall flutter. Another important parameter

in the phenomenon of stall flutter is that of flow incidence angle. The incidence angle is defined as the angle between the fluid attack angle and the blade stagger angle. This angle affects the stalling point of the blade.

With these requirements as a guideline, a blade stall flutter test facility was designed.

#### Blade Flutter Test Facility

The existing flutter rig used by Daws [8] and Sparks [9] was extensively modified in order to satisfy the requirements discussed in the previous section. To reduce disturbances in the flow, the rotor was placed at the center of the fan casing allowing a full rotor diameter, 0.20 m (8 in.) upstream and downstream to be free of flow disturbance. This required that the rotor be press fitted onto the center of a 0.58 m (23 in.) shaft. To further reduce flow disturbances, the bearing support struts were streamlined and a bellmouth was placed on the inlet of the fan as shown in Fig. 6. To obtain the speed capacity necessary to investigate stall flutter under varying conditions, a Vickers 3600 RPM, 30.5N·m (270 in.lb) hydraulic motor was chosen to drive the fan through a 2.77 ratio Browning gear belt speed increaser as seen in Figs. 7 and 8. Using the speed increaser, speeds of up to 10,000 RPM were obtainable. A hydraulic motor was chosen because a hydraulic source pump was already available at the research site. Variable speeds were obtained by shunting the fluid across the motor through a regulating valve. Rotational speed of the fan was displayed on a Keithley 168 Autorange digital voltmeter. One volt D.C. represented 1,000 RPM. The D.C. voltage was supplied from a

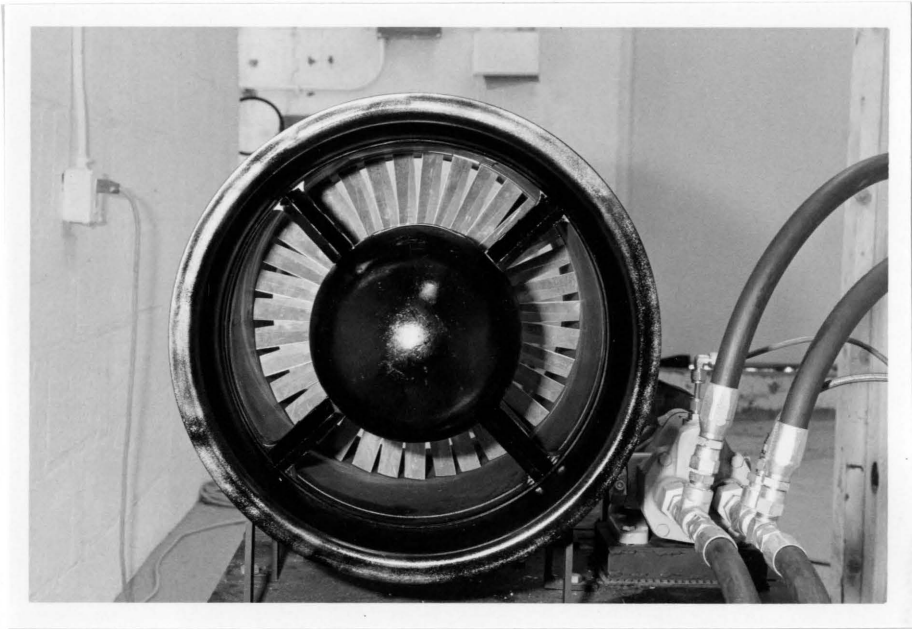


FIGURE 6. VIEW OF INLET OF TEST FAN



FIGURE 7. VIEW OF DRIVE SYSTEM ON TEST FAN

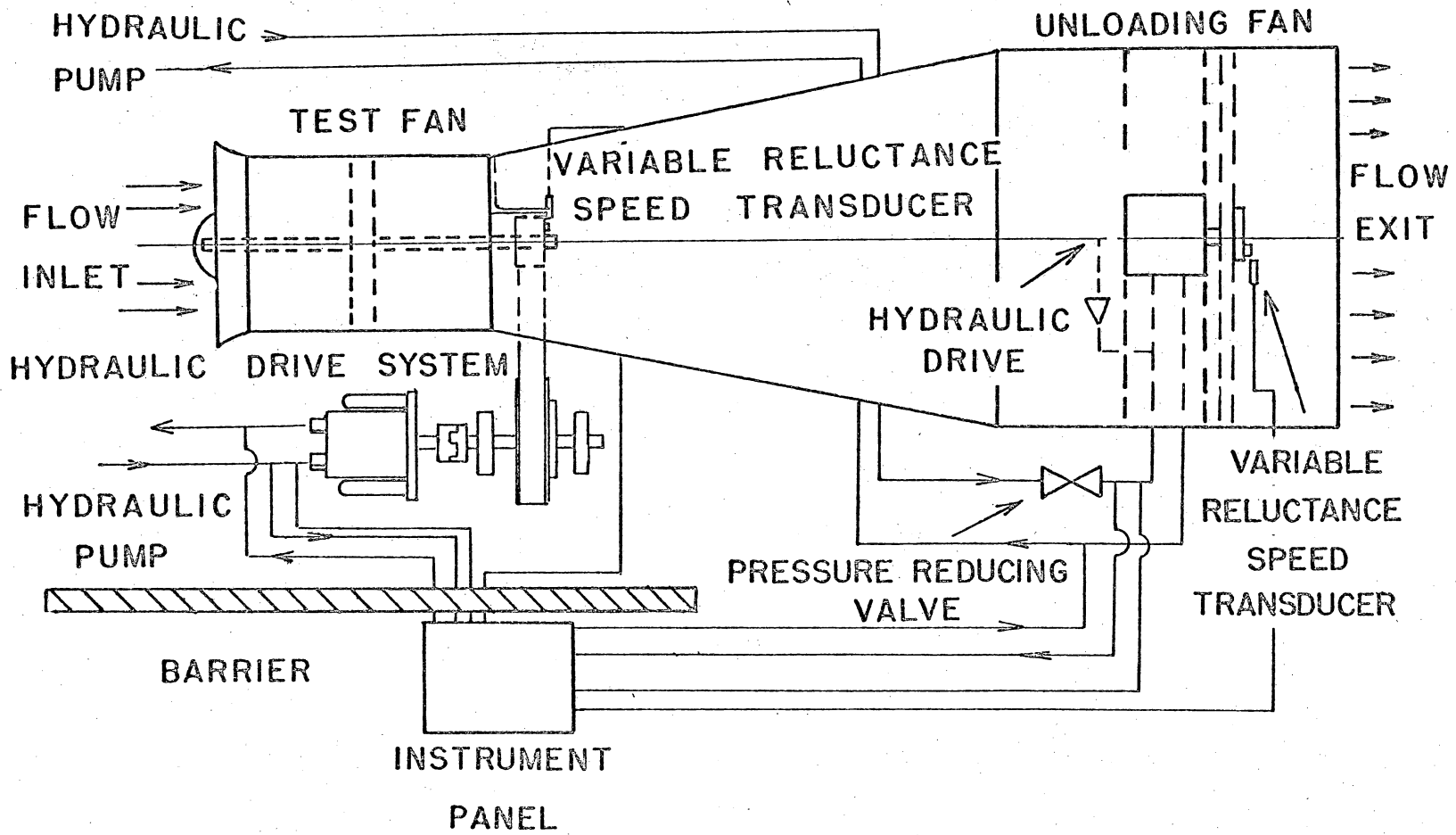


FIGURE 8. FLUTTER TEST FACILITY SCHEMATIC

variable reluctance transducer which provided a 2 volt pulse per revolution for a Teledyne-Philbrick 4702 frequency-to-voltage converter.

The fan shaft was supported by two Fafnir composite-ring ball bearings mounted 0.4 m (16 in.) between centers. The shaft supported the 0.20 m (8 in.) diameter rotor with 35 blades. The outer rotor diameter was 0.28 m (11 in.), giving a hub-to-tip ratio of 0.72. The rotor was designed to accommodate variable blade stagger angles from 0 to 65 degrees. To aid in the changing of stagger angle, a hatch was cut in the casing and inner annulus as shown in Fig. 9. The rotor solidity was set at 1 through the use of 35 blades spaced 1 inch apart at mid-span. These blades were fabricated from Alclad 2024 T3 aluminum. The blades were 76.2 mm (3 in.) in length, 25.4 mm (1 in.) in chord, and 0.40 mm (0.016 in.) in thickness. Fig. 10 shows a single blade.

For future research on the effect of incidence angle on stall flutter, an Aerovent direct-drive tubeaxial fan, driven by a Vickers vane type hydraulic motor was installed at the exit of the test fan. The fan will be used for varying the incidence of the flow in the test fan during operation.

#### Photographic Method

To investigate the use of photographic techniques in stall flutter measurements, this method was used instead of previous F.M. Telemetry methods, although the test facility is designed to accommodate telemetry methods.

Photographs of rotating blades were obtained using a 35 mm Nikon camera outfitted with a bellows focusing attachment and a 300 mm f4.5



FIGURE 9. VIEW OF HATCH TO AID IN VARYING BLADE STAGGER ANGLE



FIGURE 10. VIEW OF TEST FAN BLADE

Auto Nikkor lens. The camera was positioned 1.5 m (5.0 ft) from the leading edge of the blade so that little inlet distortion was produced in the test fan by the camera equipment. The light source for this photography was provided by a General Radio strobolume. The photographic system is shown in Fig. 11. Photographs were taken by opening the camera shutter in total darkness and illuminating the blades with a 33 microsecond pulse of light from the strobolume. This procedure does not allow for continuous investigation of one blade. Therefore, multiple photographs were taken to assure capture of a vibrating blade on film.

A viewport to provide for photographs of the tips of the blades through the casing was also designed but was not employed in this investigation.

#### Acoustical Method

To aid in the identification of flutter, a B & K sound level meter was placed near the inlet of the fan to monitor the audible change in tone at the onset of flutter. The sound level meter signal was monitored on a Tektronix oscilloscope. A Spectral Dynamics Model SD330A real-time analyzer (RTA) was also used to monitor the signal and display its frequency content. The oscilloscope and RTA data were recorded with a Tektronix type C-12 oscilloscope camera. This instrumentation is shown in Fig. 12.

#### Flow Measurement

The test fan axial velocity was measured at a point 35.5 mm (1.4 in.) upstream of the leading edge of the blade with a United Sensor DC-125 yaw



FIGURE 11. VIEW OF PHOTOGRAPHIC EQUIPMENT



FIGURE 12. VIEW OF TEST FAN INSTRUMENTATION

probe. This pressure was displayed in inches of water on a F.W. Dwyer Magnehelic pressure gauge.

## RESULTS

### Experimental Procedure

To investigate stall flutter in the experimental fan, a procedure was developed such that the flutter speed for variable stagger angles could be determined and a permanent photographic and sonic record of the occurrence obtained. Due to the late availability of the drive motor for the unloading fan, the effect of incidence angle on stall flutter was not investigated.

The experimental procedure used involved decreasing the blade stagger angle in steps of 5 degrees from a starting value of 65 degrees, which was the maximum obtainable stagger angle on the experimental fan. For each stagger angle the test fan speed was increased from zero until flutter was detected by the sonic measurement system. Detection of flutter was noted by the sharp increases and decreases in amplitude of the sound level meter output. At this point the test fan rotational speed and inlet dynamic pressure were recorded. The speed was then reduced below the flutter speed and photographs of the blades were taken. At this speed, a photograph of the sound level meter and variable reluctance speed transducer output was taken from the oscilloscope. The speed transducer output was used to obtain a permanent record of the speed at which the photographs were taken. The fan rotational speed was then increased above the flutter speed to a point where the sound level meter output was steady. At this speed flutter was continuously evident, therefore increasing the possibility of photographing a blade that was vibrating. While the photographs were taken, the sonic frequency content of the

sound level meter output was averaged and recorded from the RTA. The sound level meter and variable reluctance speed transducer output were also recorded for comparison with the previous non-flutter speed sonic output. This procedure was followed for 5-degree reductions of stagger angles to 40 degrees. At a stagger angle of 40 degrees, flutter was not detected up to a rotational speed of 4,000 RPM. Therefore, to prevent blade bending, the procedure was halted at this point until the unloading fan installation was complete.

#### Experimental Results

Analysis of the inlet flow measurements through the use of velocity triangles as shown in Fig. 13 determines the incidence angle at the onset of flutter. The flow incidence angle and rotational speed at the onset of flutter, which were experimentally determined for stagger angles between 65 and 45 degrees, appear in Table 1. Fig. 14 shows the effect of stagger angle on rotor speed at which flutter was noted. Using the flow information shown in Table 1, the relative velocity over the blades was calculated for the flutter point. This information is shown plotted as a function of blade stagger angle in Fig. 23 of Appendix 2. Photographs of the fan blades and sound level meter outputs before and during flutter are presented in Figs. 15 through 22 to verify the evidence of the flutter phenomenon. A frequency analysis of the fan sonic output during flutter for the stagger angles investigated is shown in Fig. 24 of Appendix 2.

TABLE 1. STALL FLUTTER SPEED AND INCIDENCE ANGLE COMPARISONS

Stagger Angle, Degrees	Inlet Velocity, m/sec (ft/sec)	Blade Midspan Velocity m/sec (ft/sec)	Flow Incidence Angle, Degrees	Flutter Speed, RPM
65	15.5 (51)	36.6 (120)	2	2500
60	17.7 (58)	35.1 (115)	3	2400
55	17.1 (56)	32.3 (106)	7	2200
50	16.4 (54)	29.3 (96)	11	2000
45	15.5 (51)	29.3 (96)	17	2000

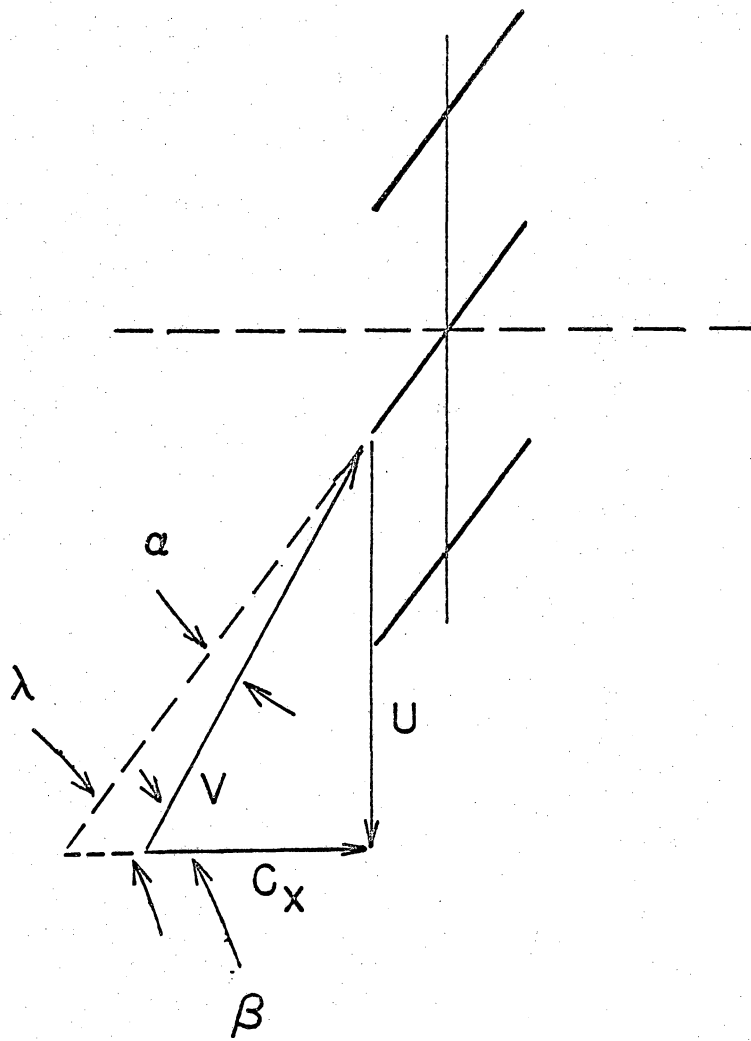


FIGURE 13. VELOCITY TRIANGLE

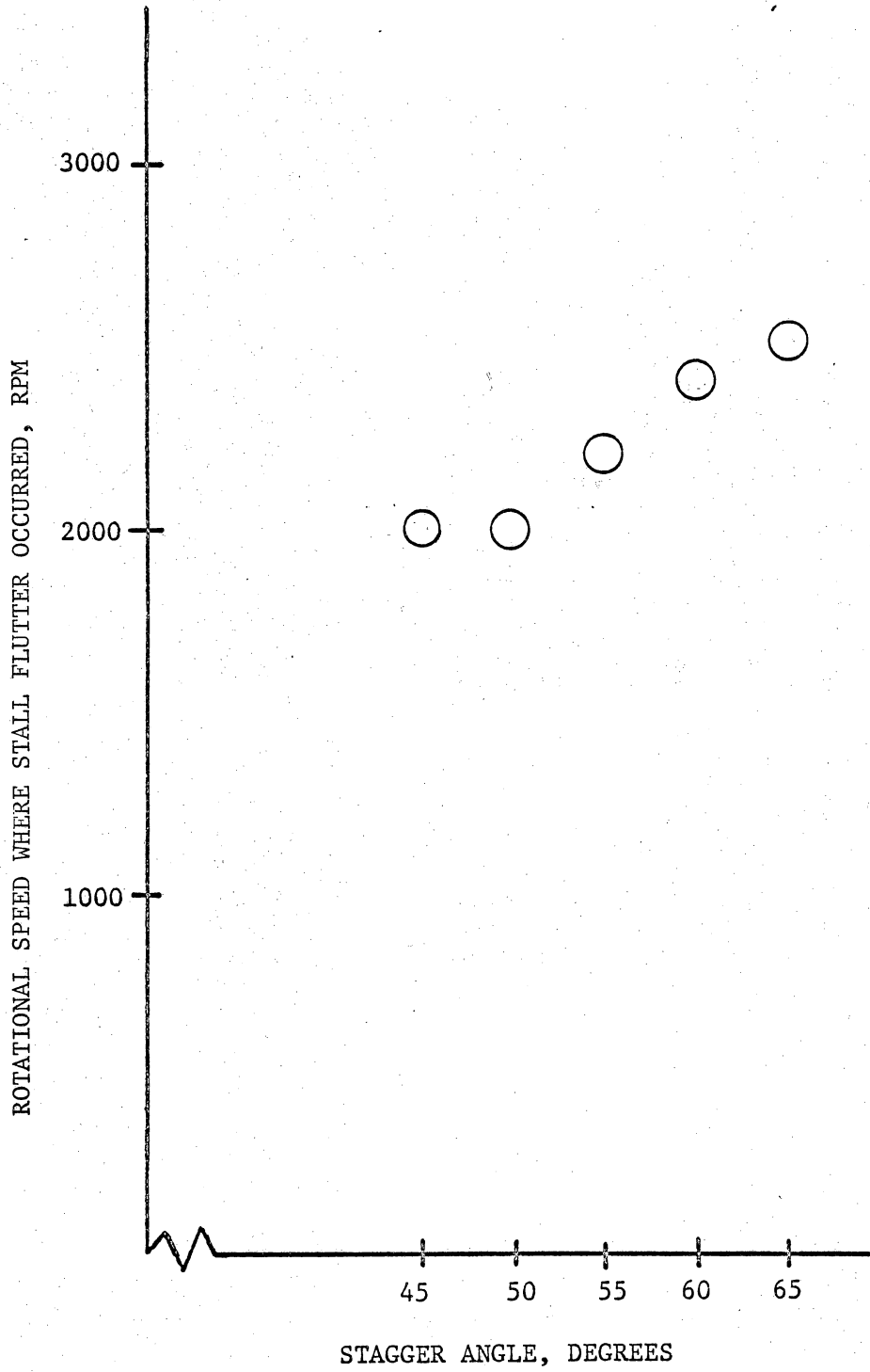
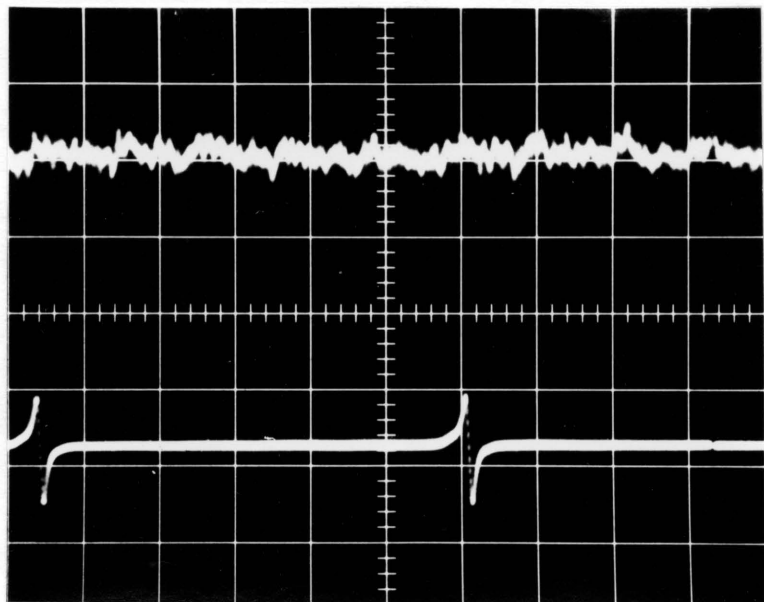
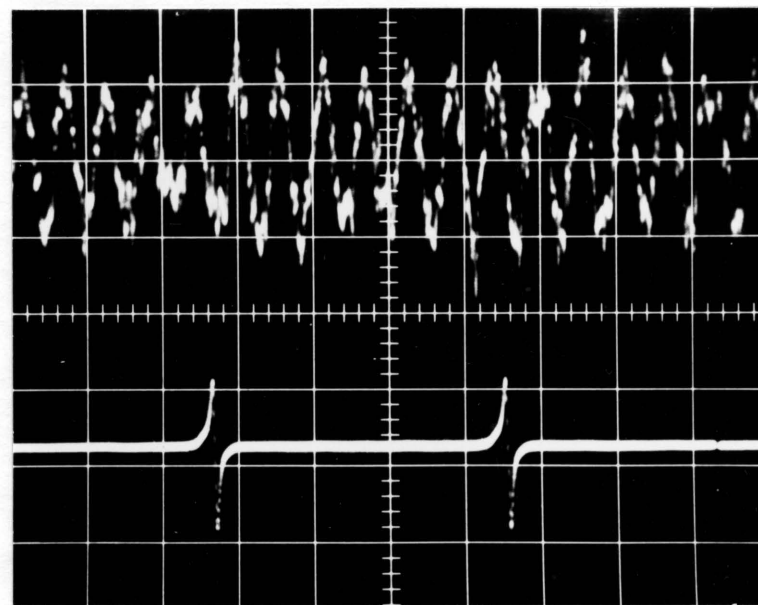


FIGURE 14. STALL FLUTTER SPEED COMPARISON



2000 RPM



3000 RPM

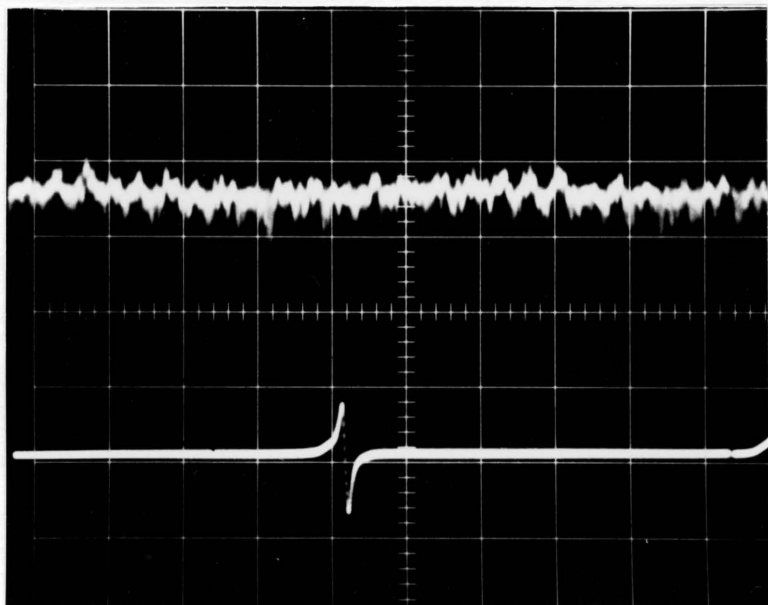
VERTICAL AXIS:

TOP TRACE - SOUND LEVEL OUTPUT, 2 VOLTS PER MAJOR DIVISION

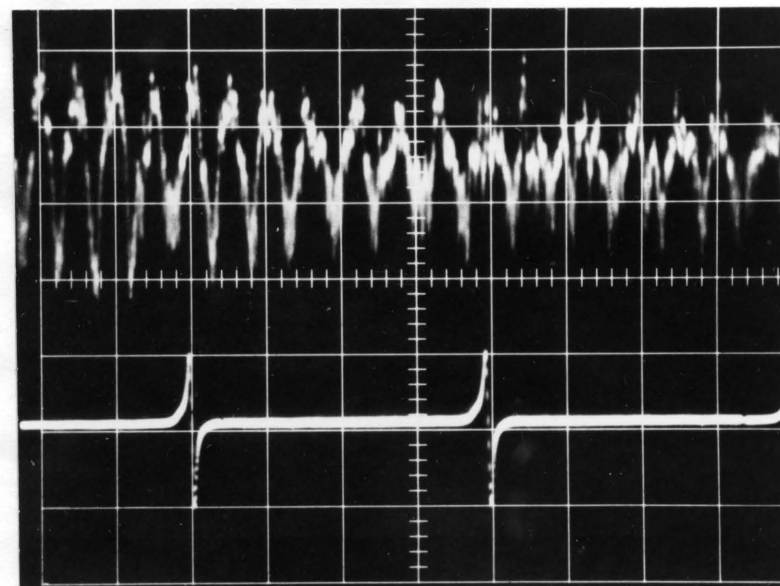
BOTTOM TRACE - SPEED TRANSDUCER OUTPUT, 2 VOLTS PER MAJOR DIVISION

HORIZONTAL AXIS: TIME, 0.005 SEC PER MAJOR DIVISION

FIGURE 15. COMPARISON BETWEEN SONIC WAVEFORM AT 2000 RPM AND 3000 RPM (FLUTTER PRESENT)  
WITH A 65-DEGREE BLADE STAGGER ANGLE



2000 RPM



3000 RPM

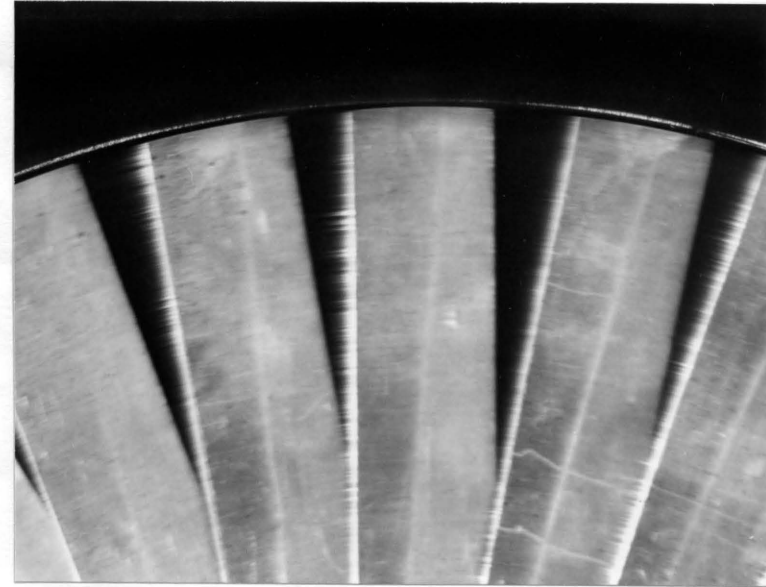
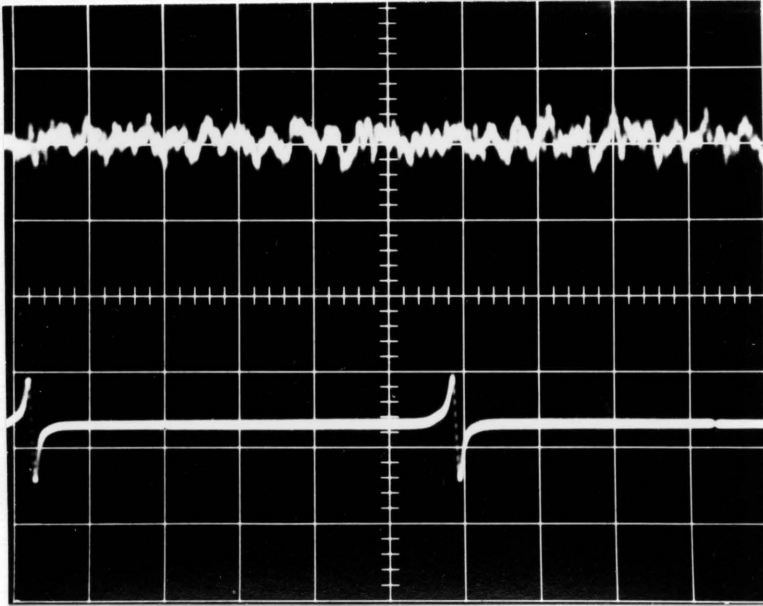
VERTICAL AXIS:

TOP TRACE - SOUND LEVEL OUTPUT, 2 VOLTS PER MAJOR DIVISION

BOTTOM TRACE - SPEED TRANSDUCER OUTPUT, 2 VOLTS PER MAJOR DIVISION

HORIZONTAL AXIS: TIME, 0.005 SEC PER MAJOR DIVISION

FIGURE 16. COMPARISON BETWEEN SONIC WAVEFORM AT 2000 RPM AND 3000 RPM (FLUTTER PRESENT)  
WITH A 60-DEGREE BLADE STAGGER ANGLE



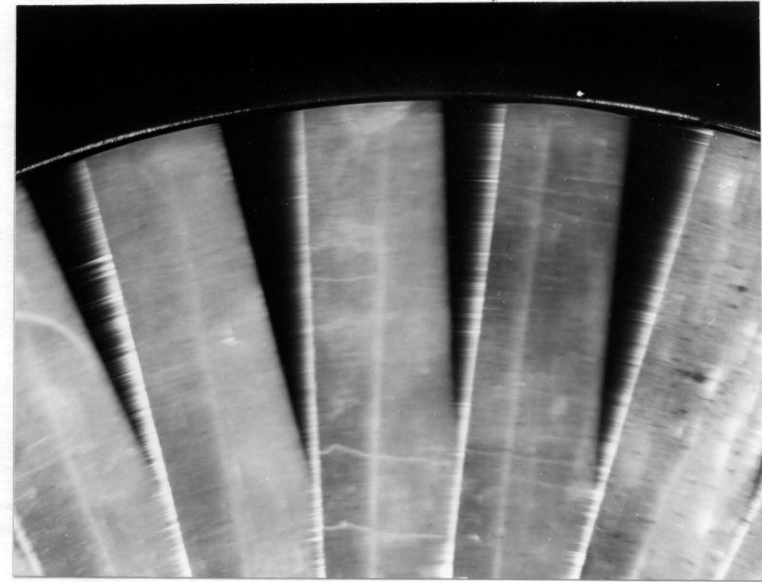
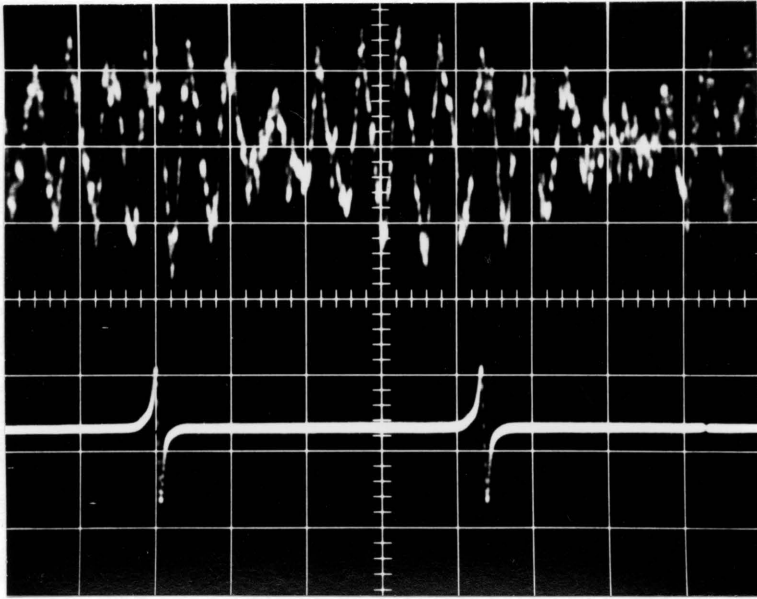
VERTICAL AXIS:

TOP TRACE - SOUND LEVEL OUTPUT, 2 VOLTS PER MAJOR DIVISION

BOTTOM TRACE - SPEED TRANSDUCER OUTPUT, 2 VOLTS PER MAJOR DIVISION

HORIZONTAL AXIS: TIME 0.005 SEC PER MAJOR DIVISION

FIGURE 17. SONIC WAVEFORM AND BLADE PHOTOGRAPH  
AT 2100 RPM FOR BLADE STAGGER ANGLE OF 55 DEGREES

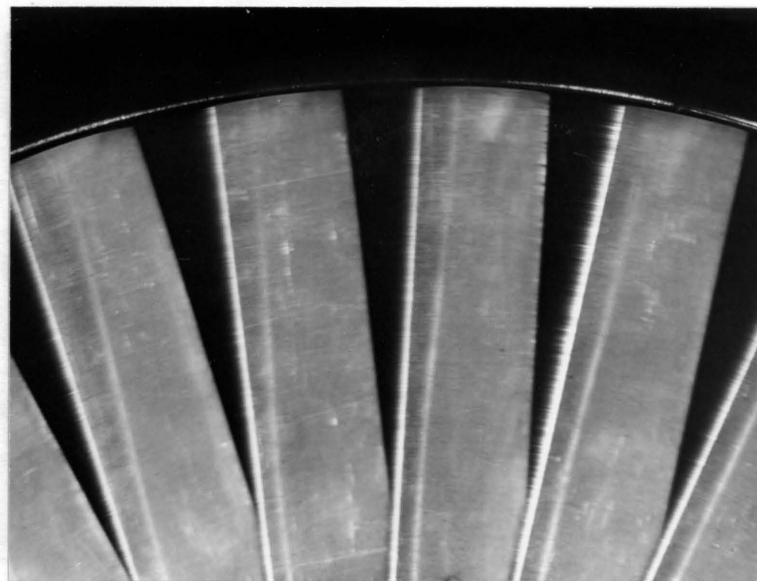
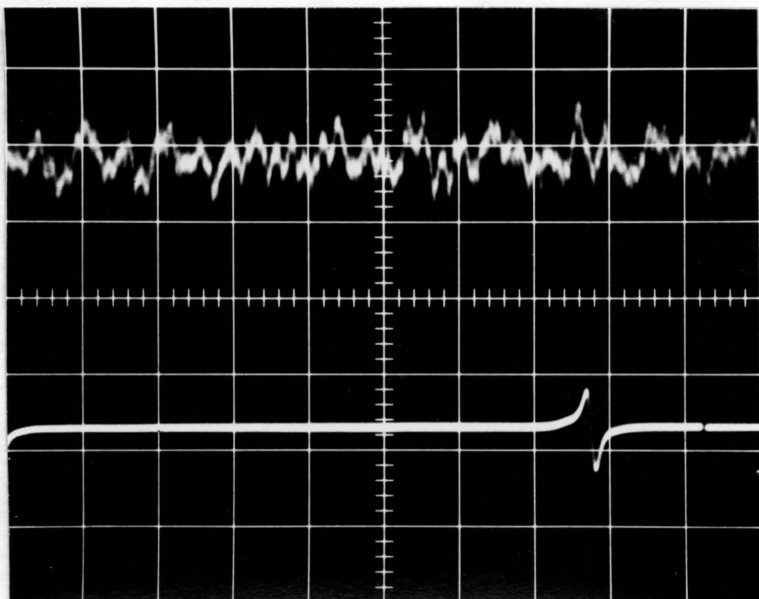


VERTICAL AXIS:

TOP TRACE - SOUND LEVEL OUTPUT, 2 VOLTS PER MAJOR DIVISION  
BOTTOM TRACE - SPEED TRANSDUCER OUTPUT, 2 VOLTS PER MAJOR DIVISION

HORIZONTAL AXIS: TIME 0.005 SEC PER MAJOR DIVISION

FIGURE 18. SONIC WAVEFORM AND BLADE PHOTOGRAPH  
AT 2800 RPM FOR A BLADE STAGGER ANGLE OF 55 DEGREES  
(FLUTTER PRESENT)

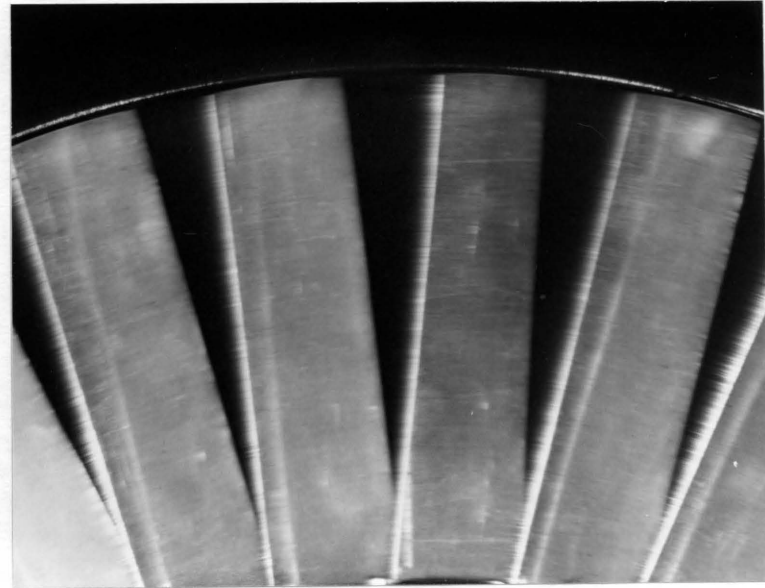
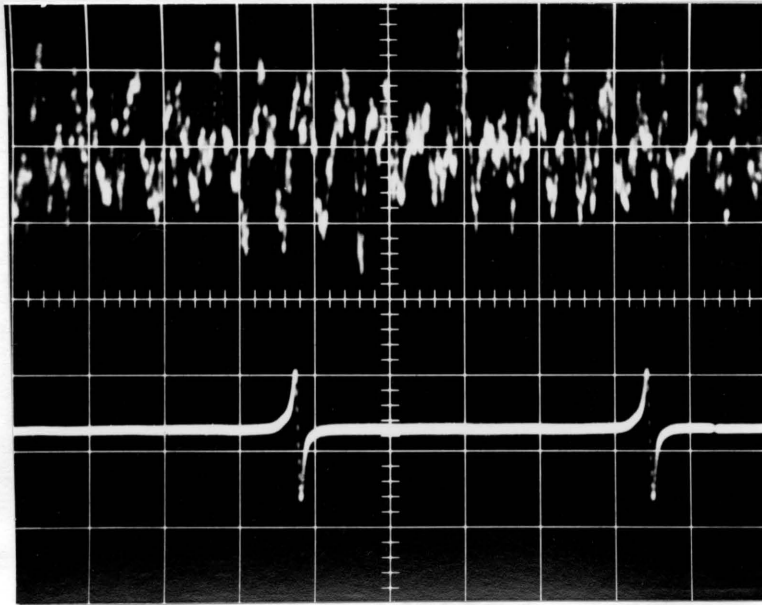


VERTICAL AXIS:

TOP TRACE - SOUND LEVEL OUTPUT, 2 VOLTS PER MAJOR DIVISION  
BOTTOM TRACE - SPEED TRANSDUCER OUTPUT, 2 VOLTS PER MAJOR DIVISION

HORIZONTAL AXIS: TIME 0.005 SEC PER MAJOR DIVISION

FIGURE 19. SONIC WAVEFORM AND BLADE PHOTOGRAPH  
AT 1500 RPM FOR A BLADE STAGGER ANGLE OF 50 DEGREES



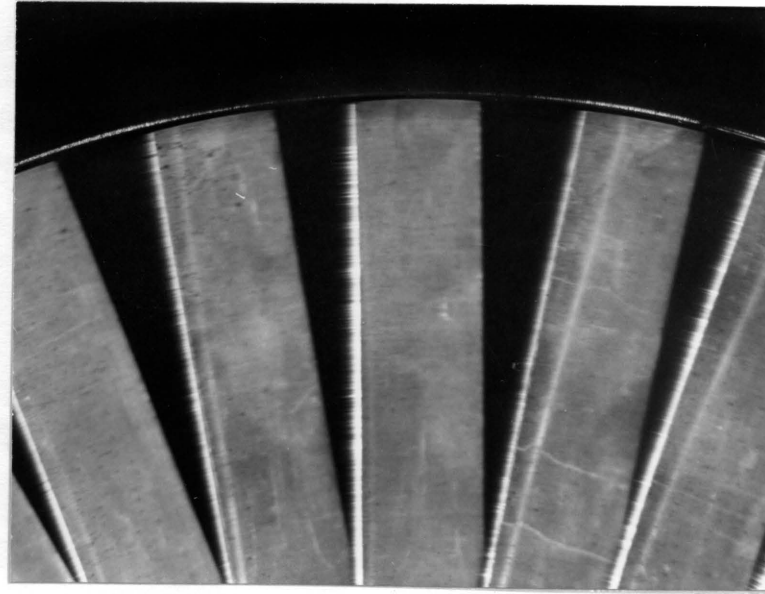
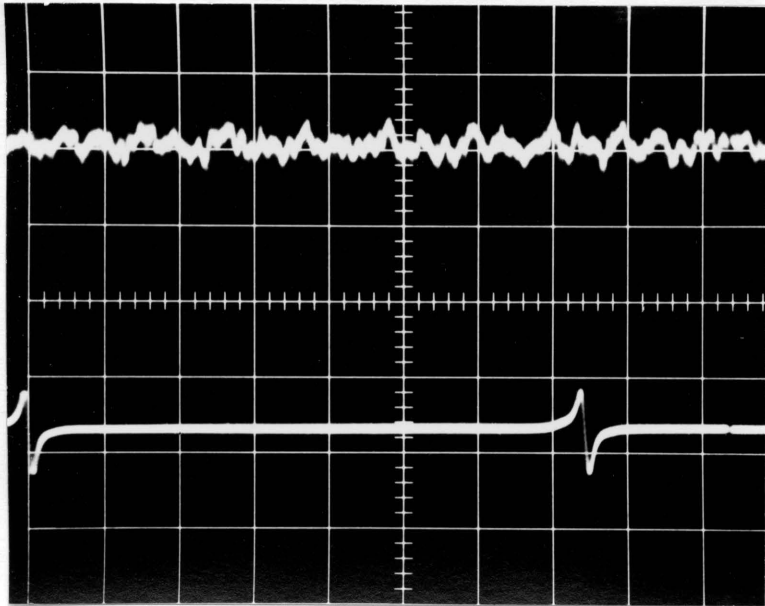
VERTICAL AXIS:

TOP TRACE - SOUND LEVEL OUTPUT, 2 VOLTS PER MAJOR DIVISION  
BOTTOM TRACE - SPEED TRANSDUCER OUTPUT, 2 VOLTS PER MAJOR DIVISION

HORIZONTAL AXIS: TIME 0.005 SEC PER MAJOR DIVISION

FIGURE 20. SONIC WAVEFORM AND BLADE PHOTOGRAPH  
AT 2500 RPM FOR A BLADE STAGGER ANGLE OF 50 DEGREES

(FLUTTER PRESENT)

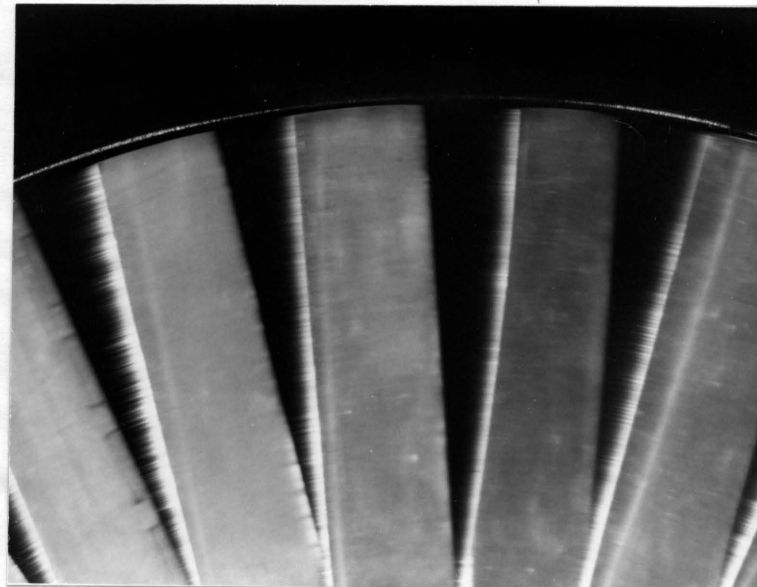
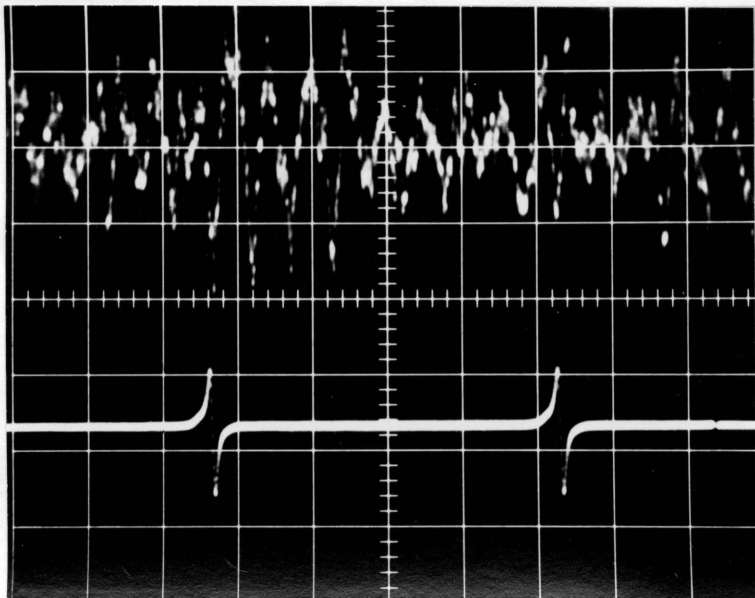


VERTICAL AXIS:

TOP TRACE - SOUND LEVEL OUTPUT, 2 VOLTS PER MAJOR DIVISION  
BOTTOM TRACE - SPEED TRANSDUCER OUTPUT, 2 VOLTS PER MAJOR DIVISION

HORIZONTAL AXIS: TIME 0.005 SEC PER MAJOR DIVISION

FIGURE 21. SONIC WAVEFORM AND BLADE PHOTOGRAPH  
AT 1600 RPM FOR A BLADE STAGGER ANGLE OF 45 DEGREES



VERTICAL AXIS:

TOP TRACE - SOUND LEVEL OUTPUT, 2 VOLTS PER MAJOR DIVISION  
BOTTOM TRACE - SPEED TRANSDUCER OUTPUT, 2 VOLTS PER MAJOR DIVISION

HORIZONTAL AXIS: TIME 0.005 SEC PER MAJOR DIVISION

FIGURE 22. SONIC WAVEFORM AND BLADE PHOTOGRAPH  
AT 2500 RPM FOR A BLADE STAGGER ANGLE OF 45 DEGREES  
(FLUTTER PRESENT)

## DISCUSSION OF RESULTS

The evidence that stall flutter was achieved in an experimental fan with 35 flat plate rectangular blades is as listed below.

(1) The stall flutter phenomenon is primarily associated with blade vibrations that are torsional in nature, as stated by Y. C. Fung [15]. The theoretical torsional natural frequency of the test blades, as determined from R. J. Roark's [16] cantilevered beam model, was 324 Hz. Fig. 24 of Appendix 2 shows that the major frequency component of the sonic output during flutter was 348 Hz. The frequency analysis of the fan sonic output cannot be precisely related to the blade vibratory frequencies due to the difference in reference frames. The sound level meter is in a stationary reference frame while the blades are vibrating in a rotational frame. A shift in apparent blade vibratory frequency measured by the sound level meter can be expected. This frequency is within 7 percent of the theoretical torsional natural frequency, therefore indicating torsional blade oscillations during flutter. These torsional oscillations indicate the presence of stall flutter.

(2) The photographs of the fan blades during flutter shown in Figs. 18, 20 and 22 also indicate torsional blade motion, again supporting the evidence of stall flutter.

(3) The incidence angle data determined from inlet flow measurements during flutter shown in Table 1 indicate stalled flow on the blades. A two-degree incidence angle would not normally indicate stall on a cambered blade. Therefore, at this point it is assumed that there are sufficient losses to cause stall on blades with zero camber for a two-degree incidence angle. A more detailed investigation of losses

would be necessary to verify this assumption. The blades are certainly stalled at stagger angles of 45 and 50 degrees due to flow incidence angles greater than 10 degrees.

With the presence of stall flutter verified, further discussion of the phenomenon can be made.

Table 1 shows that the flow incidence angle increases as stagger angle is reduced. During the experimental procedure it was noted that the regularity of the characteristic sound during flutter decreased with reduction of stagger angle. At 45 degrees the characteristic sound output was very sporadic. Fig. 24 of Appendix 2 shows the reduction in average amplitude of the dominant frequency component, of the sonic output during flutter, with decreasing stagger angle. It appears that there is a point in the reduction of stagger angle below which the blades become severely stalled and flutter cannot be achieved. In this fan, stall flutter was not evident for stagger angles below 45 degrees. From Table 1 it can be seen that at a stagger angle of 45 degrees the incidence angle was recorded as 17 degrees. Therefore, for incidence angles greater than 17 degrees the blades become completely stalled and do not oscillate torsionally in and out of stall, as for the lower incidence angles, and stall flutter is not evident. The addition of the loading fan to the test fan will greatly enhance the investigative capabilities of the effect of incidence angle on stall flutter. Table 1 also shows that the flutter speed of this experimental fan decreased with decreasing stagger angles until the incidence angle became too great for stall flutter to occur. This decrease in flutter speed with decreasing stagger angle correlates with Sparks' [9] results. Fig. 23 shows that the flow

velocity relative to the blade chord at the onset of flutter decreases with decreasing stagger angle. It is contradictory to the analytic results for a cascade of rotor blades reported by White [17]. White reports an increase in flutter relative velocity with a decrease in stagger angle from 60 degrees to 45 degrees.

Photographs of the blades during stall flutter shown in Figs. 18, 20 and 22 indicate that an interblade phase angle during stall flutter is evident. These figures show that one blade may be twisted during stall flutter, while blades on either side of it remain in an undeflected position. Photographs of stall flutter for stagger angles of 65 and 60 degrees are not presented because the foreshortening of the blade chord during torsional vibration as viewed by the camera was too small to observe. Fig. 24 of Appendix 2 shows that the flutter frequency does not vary significantly with stagger angle.

#### Summary of Results

An experimental fan was constructed that would generate stall flutter in the blading at relatively low rotational speeds. The existence of stall flutter was indicated through incidence angle investigations, photography and sonic waveform analysis. Photographic results showed that there was a finite interblade phase angle during stall flutter. It was also determined that the flutter frequency remained constant near the torsional natural frequency of the blades while the stagger angle was reduced. The flutter speed decreased with decreasing stagger angle.

## CONCLUSIONS

- (1) Stall flutter can be obtained in the tested experimental fan with 35 flat plate rectangular blades.
- (2) Stall flutter can be recorded through photographic methods at the compressor inlet for stagger angles below 60 degrees.
- (3) During stall flutter an interblade phase angle between adjacent blades is evident.
- (4) Flow incidence angle affects the characteristics of stall flutter.
- (5) Acoustical information can be used to determine stall flutter frequency, which was found to be within 7 percent of the theoretical torsional natural frequency of the blades.

## RECOMMENDATIONS

- (1) Further studies of flutter-related flow and blade parameters should be performed since the development of an experimental facility for stall flutter research has been achieved.
- (2) On-rotor measurements on adjacent blades during stall flutter should be implemented to aid in the development of and improvements in analytical prediction methods.
- (3) A high speed motion picture of stall flutter in this experimental fan is desirable to increase the understanding of the phenomenon.
- (4) Tip photography should be developed to aid in the investigation of stall flutter at stagger angles greater than 60 degrees.
- (5) Further investigation into the effects of cascade solidity on flutter speed should be undertaken.

LITERATURE CITED

- [1] Mikolajczak, A. A., Arnoldi, R. A., Snyder, L. E. and Stargardter, H., "Advanced in Fan and Compressor Blade Flutter Analysis and Predictions", Journal of Aircraft, Vol. 12, No. 4, April, 1975.
- [2] Tikhonov, N. D., "Influence of the Geometrical Parameters of the profile and Cascade on the Critical Flutter Velocity of a Pack of Compressor Blades", in Strength of Materials, Vol. 6, No. 8, Aug., 1974.
- [3] Carta, F. O. and St. Hilaire, A. O., "Experimentally Determined Stability Parameters of a Subsonic Cascade Oscillating Near Stall", ASME Paper No. 77-GT-47, 1977.
- [4] Yashima, S. and Tanaka, H., "Torsional Flutter in Stalled Cascade", ASME Paper No. 77-GT-72, 1977.
- [5] Hockley, B. S., Ford, R. A. J. and Foord, C. A., "Measurement of Fan Vibration Using Double Pulse Holography", ASME Paper No. 78-GT-111, 1978.
- [6] Jeffers II, J. D. and Meece, Jr., C. E., "F100 Fan Stall Flutter Problem Review and Solution", Journal of Aircraft, Vol. 12, No. 4, 1975.
- [7] Banerjee, S. and Rao, J. S., "Coupled Bending-Torsion Vibrations of Rotating Blades", ASME Paper No. 76-GT-43, 1976.
- [8] Daws, J. W., "An Experimental and Analytical Investigation of Bending Torsional Flutter of a Rotating Uniform Cross-Section Rectangular Blade", M.S. Thesis, Virginia Polytechnic Institute and State University, 1974.
- [9] Sparks, J. F., "The Flutter of Uniform Cross-Section Rectangular Blades with Emphasis on Experimentally Determined Rotating Cascade Effects", M.S. Thesis, Virginia Polytechnic Institute and State University, 1975.
- [10] Adler, A., "Telemetry for Rotating Measurements on Turbomachinery", ASME Paper No. 78-GT-105, 1978.
- [11] Stargardter, H., "Optical Determination of Rotating Fan Blade Deflections", ASME Paper No. 76-GT-48, 1976.
- [12] Bien, F. and Camac, M., "An Optical Technique for Measuring Vibratory Motion in Rotating Machinery", AIAA Journal, Vol. 15, No. 9, Sept., 1977.

- [13] Nieberding, W. C. and Pollack, J. L., "Optical Detection of Blade Flutter", NASA Technical Memorandum X 73573, No. 77N20108, 1977.
- [14] Schnittger, J. R., "The Stress Problem of Vibrating Compressor Blades", Journal Applied Mechanics, Vol. 22, No. 1, 1955, pp. 57-64.
- [15] Fung, Y. C., An Introduction to the Theory of Aeroelasticity, Dover Publications, Inc., New York, 1969, p. 332.
- [16] Roark, R. J. and Young, W. C., Formulas for Stress and Strain, McGraw-Hill Book Co., New York, 1975, p. 578.
- [17] White, G. P., "Flutter Analysis of a Cascade of Rotor Blades", AIAA Technical Paper No. 77-308, January 1977.

APPENDIX 1

LIST OF EQUIPMENT

<u>Item</u>	<u>Manufacturer</u>	<u>Mod. No.</u>	<u>Ser. No.</u>
Sound Level Meter	B & K	1613	300743
Oscilloscope Camera	Tektronix	C-12	007322
Oscilloscope	Tektronix	3A72 2B67	010883 028127
Digital Voltmeter	Keithley	168	37276
Real-time Analyzer	Spectral Dynamics	SD 330A	251
Magnehelic Pressure Gage	F. W. Dwyer	----	70203JP86 70220JP90
Yaw Probe	United Sensor	DC-125	B11205
35 mm Camera	Nikon-F	1500	7160006
Tripod	Gitzo	323	----
Bellows Focusing Attachment	Nikon	PB-5	----
300 mm f4.5 lens	Auto Nikkor	H	418320
Strobolume	General Radio	1532-D	1897

APPENDIX 2

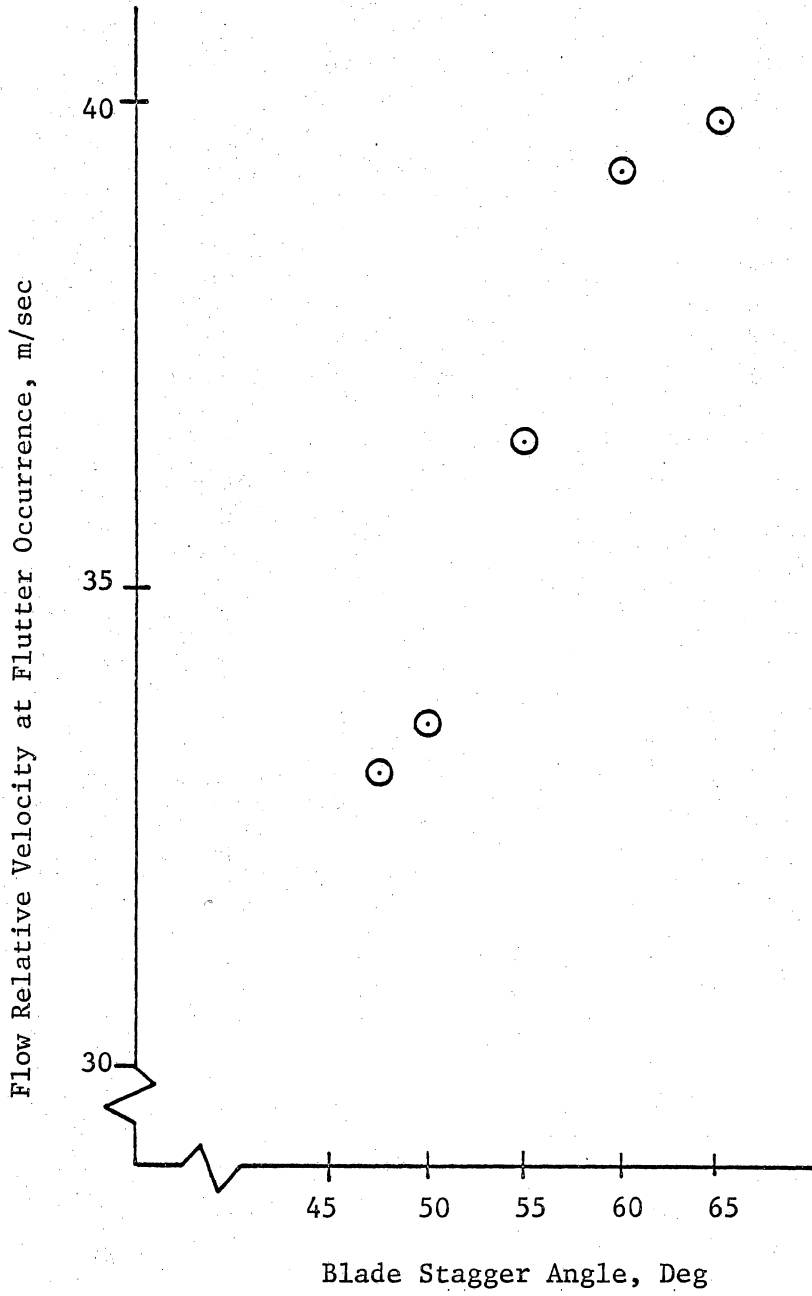
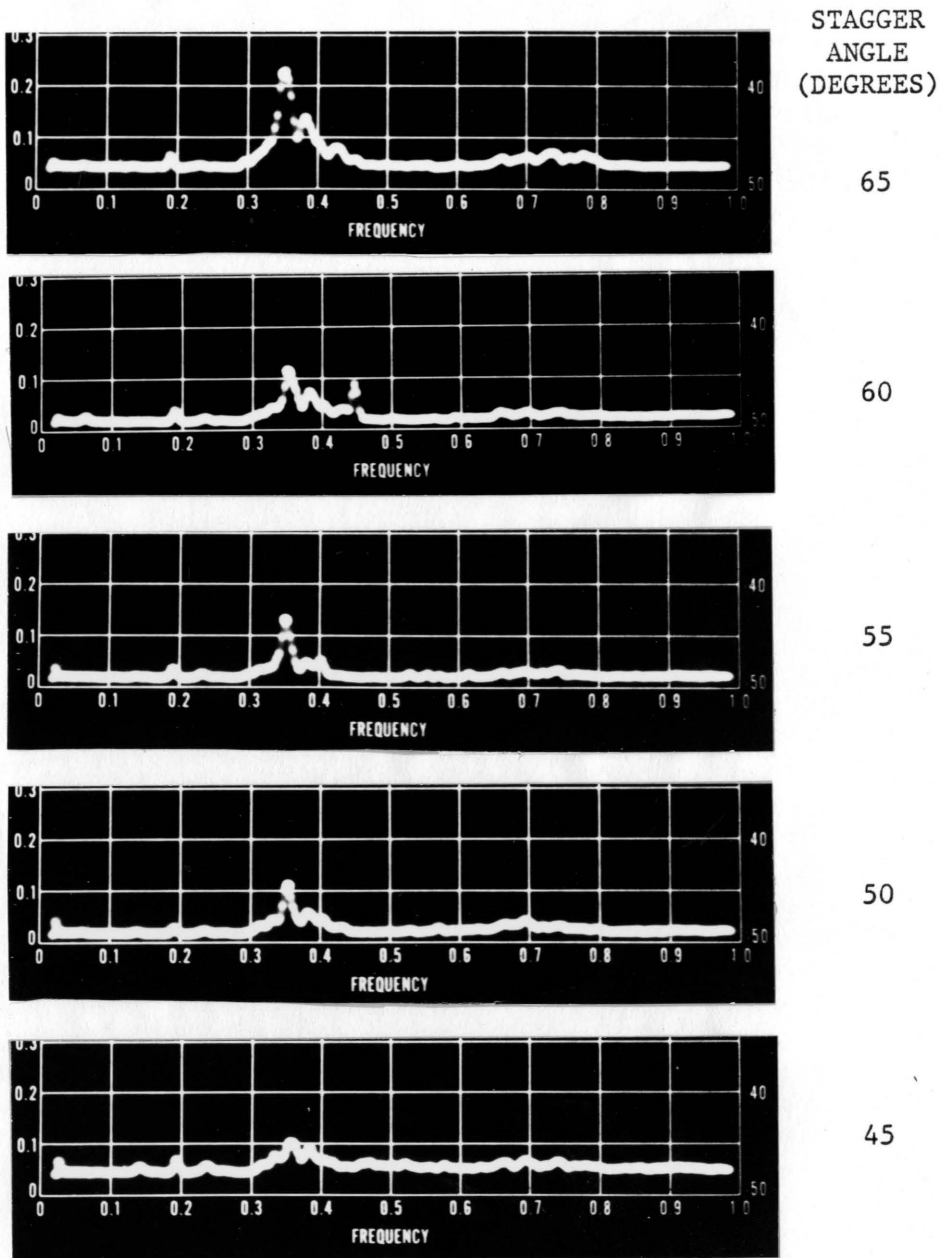


FIGURE 23. FLOW RELATIVE VELOCITY COMPARISON



VERTICAL AXIS: RELATIVE AMPLITUDE

HORIZONTAL AXIS: FREQUENCY, 100 Hz PER MAJOR DIVISION

FIGURE 24. FREQUENCY COMPONENTS OF TEST FAN SONIC OUTPUT

**The vita has been removed from  
the scanned document**

AN EXPERIMENTAL METHOD FOR THE INVESTIGATION  
OF SUBSONIC STALL FLUTTER IN GAS TURBINE ENGINE FANS  
AND COMPRESSORS

by

William W. Copenhaver

(ABSTRACT)

A facility for the investigation of stall flutter in aircraft engine compressors and fans was designed. Stall flutter was achieved in the test fan and verified through sonic and photographic methods. The frequency components of the sonic output during flutter were determined using a real-time analyzer. This frequency analysis indicated a dominant peak within 7 percent of the theoretical torsional natural frequency of the blades.

Photographs taken during stall flutter indicated the presence of an interblade phase angle.

The effect of blade stagger angle, flow incidence angle and solidity on flutter speed was determined.